NIH Public Access
Author Manuscript
Am J Physiol Lung Cell Mol Physiol. Author manuscript; available in PMC 2014 September 11.

Published in final edited form as:
Am J Physiol Lung Cell Mol Physiol. 2006 December ; 291(6): L1256–L1266. doi:10.1152/ajplung.00079.2006.

Contribution of T Cell Subsets to the Pathophysiology of *Pneumocystis*-Related Immunorestitution Disease

Samir P. Bhagwat[1], **Francis Gigliotti**[1,2], **Haodong Xu**[3], and **Terry W. Wright**[1,2,*]

[1]Department of Pediatrics, University of Rochester School of Medicine and Dentistry, 601 Elmwood Avenue, Rochester, NY 14642

[2]Department of Microbiology and Immunology, University of Rochester School of Medicine and Dentistry, 601 Elmwood Avenue Rochester, NY 14642

[3]Department of Pathology and Laboratory Medicine, University of Rochester School of Medicine and Dentistry, 601 Elmwood Avenue, Rochester, NY 14642

Abstract

Immune-mediated lung injury is an important component of *Pneumocystis* pneumonia (PcP)-related immunorestitution disease (IRD). However, the individual contribution of $CD4^+$ and $CD8^+$ T cells to the pathophysiology of IRD remains undetermined. Therefore, IRD was modeled in severe combined immunodeficient mice, and specific T cell depletion was used to determine how T cell subsets interact to affect the nature and severity of disease. $CD4^+$ cells were more abundant than $CD8^+$ cells during the acute stage of IRD that coincided with impaired pulmonary physiology and organism clearance. Conversely, $CD8^+$ cells were more abundant during the resolution phase following *P. carinii* clearance. Depletion of $CD4^+$ T cells protected mice from the acute pathophysiology of IRD. However, these mice could not clear the infection and developed severe PcP at later time points when a pathological $CD8^+$ T cell response was observed. In contrast, mice depleted of $CD8^+$ T cells efficiently cleared the infection, but developed more severe disease, an increased frequency of IFN-γ-producing $CD4^+$ cells, and a prolonged $CD4^+$ T cell response than mice with both $CD4^+$ and $CD8^+$ cells. These data suggest that $CD4^+$ T cells mediate the acute respiratory disease associated with IRD. In contrast, $CD8^+$ T cells contributed to neither lung injury nor organism clearance when $CD4^+$ cells were present, but instead served to modulate CD4 function. In the absence of $CD4^+$ cells, $CD8^+$ T cells produced a non-protective, pathological immune response. These data suggest that the interplay of $CD4^+$ and $CD8^+$ T cells affects the ultimate outcome of PcP-related IRD.

Keywords

Inflammation; Pulmonary Physiology; AIDS; T cells; *Pneumocystis*

Corresponding Author: Terry W. Wright, Ph.D., Department of Pediatrics, P.O. Box 850, University of Rochester School of Medicine and Dentistry, 601 Elmwood Ave., Rochester, NY 14642., TEL: (585) 275-4246, FAX: (585) 756-7780, Terry_Wright@urmc.rochester.edu.

NIH-PA Author Manuscript
NIH-PA Author Manuscript
NIH-PA Author Manuscript

NIH-PA Author Manuscript

NIH-PA Author Manuscript

NIH-PA Author Manuscript

Introduction

Pneumocystis carinii (Pc) is an opportunistic fungus that causes pneumonia in immune-compromised patients (37), including patients with acquired immune deficiency syndrome (AIDS) (29), patients undergoing chemotherapy, and patients receiving treatment with immunosuppressive drugs during organ transplantation (34). Although exposure to *Pneumocystis carinii* is nearly universal as demonstrated by the appearance of anti-*P. carinii* antibody in 85% of children by the age of 20 months (35), a period of immunosuppression is essential for the development of clinical disease (15; 34). Several studies have demonstrated a positive correlation between the degree of inflammation and the severity of disease (4; 23; 36), suggesting that the pathogenesis of PcP is primarily inflammatory in nature, in that infection with *Pneumocystis carinii* is necessary to cause pneumonia, but certain aspects of the immune response against *P. carinii* are responsible for the associated pathophysiology (30; 39). For example, AIDS patients who demonstrate a rapid recovery of $CD4^+$ T lymphocytes after institution of combined anti-retroviral therapy may develop pulmonary decompensation in response to pre-existing pulmonary infections, including *P. carinii* (26). This clinical syndrome has been termed “immunorestitution disease” (IRD) (9). At least one study that examined the number of possible cases of IRD based on the symptoms and clinical profile, suggests that IRD may be more prevalent than previously thought (9). At the onset of PcP-related IRD, patients no longer have heavy *P. carinii* infections, making it more likely that the severity of disease is directly related to the degree of immune recovery (9; 21). It is also possible that a dysregulated immune response may be a complicating factor affecting the intensity and duration of the disease. Importantly, patients who develop PcP-related IRD have a much greater mortality rate than patients with a classical AIDS-related presentation in which $CD4^+$ T cell function is severely impaired (23). AIDS-related PcP is normally associated with higher *P. carinii* burdens, but disease severity correlates with levels of certain inflammatory markers (4) indicating that immune-mediated mechanisms of lung injury are also operative in this clinical presentation of PcP. Thus, it is possible that variation in the degree of immunosuppression among AIDS patients affects their ability to mount an immune-mediated inflammatory response to *P. carinii*, and may account for variability in the physiological presentation of PcP from one AIDS patient to the next.

The immunopathogenesis of PcP is also supported by studies in animal models. In the absence of a host immune system, e.g. as in SCID mice, very little lung damage is induced by *P. carinii* infection until poorly characterized events take place during advanced stages of PcP (39). However, when the host immune system is restored by the adoptive transfer of congenic splenocytes (immunorestitution), an intense *P. carinii*- specific immune response brings about *P. carinii* clearance with the undesired consequence of severe lung damage (31; 39). While the contribution of $CD4^+$ T cells (17; 31; 33), TNF- α (7), and IL-1 (8) to *P. carinii* clearance has been established in this IRD model, the specific contributions of $CD4^+$ and $CD8^+$ T cells to the pathological response associated with IRD remains unknown. Work from several groups (17; 30) noted that the transfer of flow-sorted $CD4^+$ cells from *P. carinii*-immunized donors to heavily infected SCID mice could induce a lethal hyper-inflammatory response, suggesting that $CD4^+$ T cells could contribute to immune-mediated pathology if sensitized by prior exposure to *P. carinii*. In addition, recent studies have

NIH-PA Author Manuscript

NIH-PA Author Manuscript

NIH-PA Author Manuscript

demonstrated that the severity of IRD can be alleviated by the transfer of $CD25^+/CD4^+$T regulatory cells (18), or the delivery of viral IL-10 to the lung (32). In addition to providing more support for the immunopathogenesis of PcP, these studies also suggest that specific immune modulation could decrease the severity of PcP-related IRD.

In the CD4-depleted model of AIDS-related PcP, mice develop progressive disease that is characterized by the accumulation of $CD8^+$ T cells and PMNs in the lung (3; 39). We have demonstrated that $CD8^+$ T cells are required for maximal inflammation and lung injury, but have little effect on *P. carinii* clearance (39). It has also been demonstrated that $CD8^+$ T cells can suppress specific immune responses by helping to limit the intensity and duration of $CD4^+$ T cell responses (19). Therefore, understanding the interplay of $CD4^+$ and $CD8^+$ T cells during IRD, and how each subset contributes to clearance, injury, and/or control of inflammation is necessary to develop optimal treatment regimens for PcP-related IRD. We hypothesize that a balanced immune response consisting of both $CD4^+$ and $CD8^+$ T cells is more effective for efficiently resolving PcP-related IRD than a response dominated by either $CD4^+$ or $CD8^+$ T cells. The work described herein tests this hypothesis in vivo.

Materials and Methods

Animal Model

B6.CB17-*Prkdcscid*/SzJ (B6 SCID) female mice were purchased from The Jackson laboratory, Bar Harbor, ME. SCID mice were infected with *P. carinii f. sp. muris* by either direct inoculation or co-housing, and then immune-reconstituted with an intra-peritoneal injection of 5×10^7 splenocytes from naive C57BL/6J donor females. For direct inoculation experiments, mice were given 1×10^5 *P. carinii* cysts by the intra-nasal route, and then immune reconstituted 17 days later. For co-housing experiments, mice were housed with heavily infected SCID mice for 6 weeks prior to immune reconstitution. We have determined that both routes of exposure result in similar *P. carinii* lung burdens at the time of reconstitution. Our laboratory now routinely uses the direct inoculation method because it accelerates the infection process, and therefore requires less time to complete individual experiments. Depletion of specific lymphocyte subsets was achieved by intra-peritoneal injection of specific $CD4^+$ T cell and $CD8^+$ T cell depleting monoclonal antibodies (MAbs). Antibody injections were given one day prior to and one day after immune reconstitution. Thereafter, antibodies were administered every four days for the duration of the experiment. Reconstituted animals received either 300 μg of control rat IgG (Sigma), 300 μg of $CD4^+$ T cell-depleting MAb (clone GK1.5, ATCC TIB 207) or 250 μg of $CD8^+$ T cell-depleting MAb (clone 2.43, ATCC TIB 210). Our immune reconstitution model is described in detail elsewhere (39). On specific days mice from each group were anesthetized with pentobarbital for lung resistance and compliance measurements (see below) and further tissue analysis. All animal protocols were pre-approved by University Committee for Animal Research (UCAR) at the University of Rochester Medical Center.

Preparation of mouse *P. carinii* organisms for inoculation

P. carinii-infected CB.17 *scid/scid* mice were treated with dexamethasone ($4 mg.l^{-1}$) and tetracycline ($500 mg.l^{-1}$) in the drinking water three to seven days prior to sacrifice to

NIH-PA Author Manuscript

NIH-PA Author Manuscript

NIH-PA Author Manuscript

increase the *P. carinii* burden in the lung. The lungs were removed, and *P. carinii* were isolated from the lung tissue as previously described (38; 41). The final prep was then stained with ammoniacal silver to enumerate cysts, and Diff-Quick (Dade AG, Dudingen, Switzerland) to ensure no bacterial contamination was present. In addition, the preps were routinely plated on commercially available chocolate blood agar plates to test for the presence of other microorganisms.

Physiologic assessment of pulmonary compliance and resistance in live, ventilated mice

Dynamic lung compliance and resistance was measured in live mice using a previously described method with modifications (5; 39; 41). Mice were anesthetized by intra-peritoneal injection of 0.13 mg of sodium pentobarbital per gram body weight. A tracheostomy was performed and a 20-gauge cannula was inserted 3 mm into an anterior nick in the exposed trachea. The thorax was then opened to equalize airway and transpulmonary pressure. To assure that the mice tolerated the procedure, they were examined for spontaneous respirations before proceeding further. Mice were immediately placed into a plethysmograph designed for anesthetized mice (BUXCO Electronics Inc.), and connected to a Harvard rodent ventilator (Harvard Apparatus, Southnatick, MA). Mice were ventilated with a tidal volume of .01 ml per gram body weight at a rate of 150 breaths per minute. Respiratory flow and pressure were measured using transducers attached to the plethysmograph chamber. Data was collected and analyzed using the Biosystems XA software package (BUXCO Electronics Inc., Wilmington, NC). Dynamic lung compliance was calculated in $ml.cm^{-1}$ H_2O from the flow and pressure signals using the method by Amdur and Mead (1), and then normalized for peak body weight. Lung resistance values were calculated in cm $H_2O.ml^{-1}.sec^{-1}$ from the same input signals.

Bronchoalveolar Lavage (BAL) and Lung Tissue Preparation

BAL and lung tissue samples were obtained following dynamic compliance measurements. The chest cavity was surgically opened to expose the lungs and trachea, and the left lung lobe was tied off securely at the bronchus with surgical silk and removed with sterile scissors. The isolated lung tissue was immediately snap frozen in liquid nitrogen, and stored at -80°C for RNA isolation. The remaining lung lobes were lavaged with four, one-ml aliquots of 1X Hank's balanced salt solution (HBSS) via the tracheal cannula. Recovered lavage fluid (∼3.5 ml per mouse) was centrifuged at 250 × g for 5 min to obtain the cellular fraction, and the supernatant was removed and frozen at −80°C for subsequent enzymelinked immunosorbent assay (ELISA) analyses of cytokine/chemokine content. The cells were resuspended in fresh HBSS, enumerated, centrifuged onto glass slides, and stained with Diff-Quick for differential counting. In addition, multiparameter flow cytometric analysis was performed on BAL cells following staining with fluorochrome-conjugated antibodies. Anti-CD4-Fluorescein (clone RM4-4), and anti-CD8a-Peridinin Chlorophylla Protein (clone 53-6.7) were purchased from BD Biosciences (San Diego, CA). These MAbs were distinct from the MAbs used to deplete $CD4^+$ and $CD8^+$ T cells in vivo. At least 5,000 events per BAL sample were routinely analyzed on a FACSCalibur^{TM} cell sorter (BD Biosciences, San Jose, CA).

NIH-PA Author Manuscript

NIH-PA Author Manuscript

NIH-PA Author Manuscript

For lung tissue fixation the lungs were inflated with 15 cm gravity flow-pressure of 10% formalin (Sigma, St. Louis, MO). The lungs were fixed for 10 min under gravity flow pressure, and then carefully removed from the animal and placed in fixative for 16 h at 4°C. The lungs were rinsed, and stored at 4°C in 70% ethanol. Prior to embedding, the lower right lung lobe of each animal was removed and placed in a tissue cassette. The lobe was embedded in paraffin, and 4μM sections were cut from the tissue blocks. Slides were stained with hematoxylin and eosin to visualize lung architecture and inflammatory infiltrates. Hematoxylin-eosin-stained tissue sections were visualized under high power magnification (600X) and inflammatory cells were blindly counted by a pathologist. Ten random fields from each slide were counted with three slides per each lung sample. Results are expressed as number of inflammatory cells per field in Figures 3 and 8.

Measurement of *P. carinii* burden by quantitative real time PCR

P. carinii burden in the lungs of experimental mice was determined by real-time PCR as previously described (41). Briefly, the right lung lobes were homogenized with phosphate buffered saline (one ml of PBS per 150 mg of lung tissue) in a mechanical homogenizer. Homogenates were boiled for 15 minutes, vigorously vortexed for 2-3 minutes, and then centrifuged for 5 minutes at 12,000 × *g*. The supernatant was carefully removed and stored at -80°C for real-time PCR analysis. Boiled samples were assayed by quantitative PCR using TaqMan® primer/fluorogenic probe chemistry, and an Applied Biosystems Prism 7000 Sequence Detection System (Applied Biosystems, Foster City, CA). A primer/probe set specific for a 96 nucleotide region of the mouse-derived *P. carinii* kexin gene (22) was designed using the Primer Express software (Applied Biosystems). The sequences of the primers and probe used were as follows: forward primer, 5′-GCACGCATTTATACTACGGATGTT-3′-; reverse primer, 5′-GAGCTATAACGCCTGCTGCAA-3′; fluorogenic probe, 5′-CAGCACTGTACATTCTGGATCTTCTGCTTCC-3′. Quantitation was determined by extrapolation against standard curves constructed from serial dilutions of known copy numbers of plasmid DNA containing the target kexin sequence. Data was analyzed using the ABI Prism 7000 SDS v1.0 software (Applied Biosystems), and is reported as total kexin DNA copies per right lung.

Cytokine and Chemokine ELISAs

ELISAs were performed on the cell-free lavage fluid collected from the experimental mice. Quantikine ELISA kits for the quantitation of TNF-α, IFN-γ, RANTES and MCP-1 were purchased from R&D Systems (Minneapolis, MN). Assays were performed according to the manufacturer's instructions.

Intracellular staining of IFN-$_{\gamma}$

Cells were isolated from the lungs of experimental mice using a previously published protocol (25). Briefly, the lungs were excised, minced and dissociated by pushing through a 60-gauge stainless steel mesh screen in a total volume of 10 ml saline. 0.5-ml aliquots were stored at -80 °C for DNA isolation and kexin copy number estimation using quantitative real time PCR. One-ml aliquots were centrifuged (13,000 RPM for 10 minutes in a

NIH-PA Author Manuscript

NIH-PA Author Manuscript

NIH-PA Author Manuscript

microcentrifuge) and the supernatants were stored at -80 °C for ELISA. Remaining eight ml of lung homogenates were processed to isolate cells for FACS analysis as follows: Cells were first centrifuge at 300 xg for 10 minutes. The pellets were resuspended in five ml complete RPMI + 3% FBS + 1mg.ml-^{1} type IV Collagenase (Invitrogen Inc.) + 50 units.ml-^{1} of Dnase I (Sigma). Cells were incubated by rocking at 37 °C for one-hour in 5 % CO_2 incubator. They were first filtered through 70 μm and 40 μm filters and centrifuged at 300g for 10 minutes. The pellet was resuspended in five ml of ice-cold RBC lysis buffer (25) and incubated on ice for three minutes. Cells were washed with 20 ml complete RPMI + 3% FBS, centrifuged and the pellet was suspended in two ml of complete RPMI + 3% FBS. Aliquots were removed to perform cell counts and remaining cells were stimulated with Phorbol myristate acetate (PMA) (50 ng.ml-^{1} final concentration) and ionomycin (0.5 μg.mL^{-1} final concentration) at 37 °C for 1.5 hours before intracellular staining of IFN-γ and FACS analysis using intracellular cytokine staining kit (BD Biosciences, San Jose, CA).

Statistical Analyses

All values reported for each experimental group are mean ± 1 standard error measurement. For each individual experiment, p-values were determined by performing a one-way analysis of variance (ANOVA) with the SigmaStat® software package (Jandel Scientific, San Rafael, CA, USA). The Student-Newmann-Keuls method was used for all pair-wise multiple comparisons of experimental groups.

Results

Kinetics of T cell recruitment during PcP-related IRD

Normal naïve splenocytes were adoptively transferred into *P. carinii*-infected SCID mice, and groups of mice were sacrificed 9, 14, 21, and 28 days later. The average *P. carinii* burden of each group was determined by real-time PCR (Figure 1, parentheses), and the absolute numbers of $CD4^+$ and $CD8^+$ T cells in the BAL were enumerated by FACS analysis (Figure 1). It was evident that of the lymphocytes infiltrating the lungs of infected mice with IRD, there were more $CD4^+$ T cells than $CD8^+$ T cells at earlier time points (Figure 1, days 9 and 14; $p<0.05$). However, $CD4^+$ T cell numbers subsequently decreased with time, coincident with organism clearance from the lungs by day 28 post-reconstitution. This observation was consistent with previous studies (17; 39) showing that $CD4^+$ T cells form the main line of defense that is responsible for *P. carinii* clearance. In contrast, there were fewer $CD8^+$ T cells than $CD4^+$ T cells during the early stages of IRD (Figure 1, days 9 and 14), but their relative proportion and total numbers increased dramatically with time post-reconstitution (there were an average of 1.3×10^5 $CD8^+$ cells on day 14, 4.2×10^5 on day 21, and 3.9×10^5 cells on day 28 post reconstitution). Increased $CD8^+$ T cell numbers coincided with the resolution phase of IRD in this model. This influx of immune cells is specific to Pc-infection and immune-reconstitution since non-infected but immune-reconstituted mice did not show a significant influx of $CD4^+$ or $CD8^+$ T cells (data not shown).

NIH-PA Author Manuscript

NIH-PA Author Manuscript

NIH-PA Author Manuscript

Contribution of CD4+ T cells to acute lung injury during PcP-related IRD

To determine whether $CD4^+$ T cells contributed to the acute lung injury associated with PcP- related IRD, normal splenocytes were adoptively transferred into *P. carinii*-infected SCID mice. Experimental groups of mice were treated with control IgG or anti-CD4 MAb. Disease severity was evaluated by measuring dynamic lung compliance, lung resistance, and weight loss. Pulmonary inflammation was assessed by examining cellular infiltrates, cytokine levels, and histology. Uninfected control SCID mice did not show any signs of pulmonary disease following immune reconstitution, supporting the requirement of *P. carinii* for the generation of the pathological IRD immune response (data not shown). As expected, *Pneumocystis*-infected immune-reconstituted mice (IRD mice) mounted an intense inflammatory response against the pre-existing *P. carinii* infection, and exhibited severe abnormalities in pulmonary physiology at 14 and 21 days post-reconstitution (Figure 2A and B). In addition, the lungs of IRD mice contained significantly elevated numbers of PMNs, which is indicative of PCP-related lung injury (Figure 2C). However, by day 28 the IRD mice had nearly cleared the infection (Figure 2D), and had improved lung function (Figure 2A and B). In contrast, the CD4-depleted IRD mice were protected from the acute stage of disease occurring at 14 and 21 days post-reconstitution, but as a consequence of impaired $CD4^+$ T cell function were unable to clear the *P. carinii* infection (Figure 2D), and subsequently deteriorated at the later time points as a result of progressive PcP (Figure 2A and B). CD4-depleted IRD mice exhibited considerably better lung compliance and resistance than non-depleted IRD mice (Figure 2A and B; $p<0.05$), had fewer lung PMNs (Figure 2C), and suffered little body weight loss (data not shown). While histological evidence of severe pulmonary inflammation was obvious in the non-depleted IRD mice (Figure 3A), the CD4-depleted IRD mice displayed little evidence of lung inflammation or injury at day 14 (Figure 3B and D). Pathological scoring of lung sections confirmed that non-depleted IRD mice had much more severe pulmonary pathology than the CD4-depleted mice (Figure 3E). Analysis of BAL revealed that increased pulmonary inflammation and injury in IRD mice was associated with elevated cytokine in the lungs (Figure 4). In contrast, CD4-depletion resulted in severely impaired lung TNF, IFN γ, MCP-1 and RANTES responses at day 14 post-reconstitution (Figure 4; $p<0.05$). These data demonstrate that depletion of $CD4^+$ T cells prevents the onset of the acute stage of immune-mediated lung injury associated with IRD.

CD8+ T cells modulate CD4+ T cell-dependent acute lung injury during PcP-related IRD

To determine whether $CD8^+$ T cells contribute to the acute injury following IRD, normal splenocytes were adoptively transferred into *P. carinii*-inf*ected* SCID mice. Experimental groups of mice were treated with either control IgG or anti-CD8 MAb. Unexpectedly, the absence of $CD8^+$ T cells actually enhanced the PcP-related IRD observed at day 9 and 14 post-reconstitution. Mice depleted of $CD8^+$ T cells had significantly decreased lung compliance, increased lung resistance, and more weight loss when compared to non-depleted and CD4-depleted mice IRD mice (Figure 2A and B; $p<0.05$). At day 21 post-reconstitution, lung function measurements were similar in non-depleted and $CD8^+$ depleted mice, but by this time both groups suffered from severe disease. Surviving mice in both groups effectively cleared the *Pneumocystis carinii* infection (Figure 2D), and began to

NIH-PA Author Manuscript

NIH-PA Author Manuscript

NIH-PA Author Manuscript

show improved lung function and weight gain by day 28 post-reconstitution. CD8-depleted mice demonstrated histological patterns of pulmonary inflammation that were generally similar to non-depleted IRD mice (Figure 3C vs. 3A). Importantly, CD8-depleted IRD mice had significantly greater amounts of TNF- α, MCP-1 and RANTES (Figure 4; $p<0.05$ for each cytokine) in the BAL fluid at day 9 post-reconstitution than non-depleted IRD mice. However, the most striking finding was the greater than 5-fold increase in IFN-γ production (Figure 4B; $p<0.05$). Although the peak number of $CD4^+$ T cells in lungs of CD8-depleted and non-depleted IRD mice were similar (Figure 5, day 14), the CD8-dpeleted IRD mice exhibited an earlier increase in $CD4^+$ T cell recruitment, and a prolonged $CD4^+$ T cell response that persisted out to 28 days post-reconstitution (Figure 5). These data demonstrate that in the absence of $CD8^+$ T cells, the early pro-inflammatory $CD4^+$ T cell response is enhanced leading to more severe IRD-related pulmonary disease.

Enhanced IFN-$_\gamma$ production in CD8-depleted mice is associated with increased numbers of $CD4^+$/IFN-γ^+ T cells

In order to determine the source of elevated IFN-γ in the CD8-depleted mice, lung cells were isolated from experimental mice, stimulated with PMA and ionomycin, and stained for intracellular IFN-γ as well as surface CD4. A representative FACS histogram confirms that specific staining for surface CD4 and intracellular IFN-γ, which was blocked with non-labeled anti-IFN antibody, was achieved (Figure 6A and B). Importantly, the CD8-depleted IRD mice had significantly more $CD4^+$/IFN-γ^+ cells in the lung than the non-depleted IRD group ($1.5 \times 10^5 \pm 4.8 \times 10^4$ in CD8-depleted group vs. $1.4 \times 10^4 \pm 8 \times 10^3$ in non-depleted group, $p<0.05$) (Figure 6C). In addition, we also compared IFN-γ levels in the lung homogenates of these mice. Non-depleted mice had 330 ± 81 pg/ml of IFN-γ in their lung homogenate as compared 1773 ± 814 pg/ml of IFN-γ in CD8-depleted mice ($p<0.05$; n=3 for each group). These results were consistent with our prior results (Figure 4B). Very few $CD8^+$ or $NK1.1^+$ cells stained positive for IFN, suggesting that $CD4^+$ cells are the major source of IFN-$_\gamma$ at this time point (data not shown). Together, these data suggest that $CD8^+$ T cells modulate the nature and intensity of the $CD4^+$ T cell response to *Pneumocystis carinii*.

$CD8^+$T cells mediate damage but not *P. carinii* clearance in the absence of $CD4^+$T cells

To determine the effect $CD8^+$ T cells have on IRD in the absence of $CD4^+$ T cells, normal splenocytes were adoptively transferred into *P. carinii*-infected SCID mice. Experimental groups of mice were treated with anti-CD4 antibody or both anti-CD4 and anti-CD8 antibodies. A control group was *P. carinii*-infected, but did not receive splenocytes. Because each group lacked $CD4^+$ T cells, none of the mice cleared the *P. carinii* infection over the four-week study, and each group had similar *P. carinii* lung burdens (Figure 2C). Thus, there was no protective anti-*P. carinii* benefit associated with the presence of $CD8^+$ T cells in this model. As expected, the non-reconstituted *P. carinii*-infected mice exhibited nearly normal pulmonary function (Figure 7A and B), and no body weight loss (data not shown). By week four post reconstitution, the CD4-depleted group showed a significant accumulation of $CD8^+$ T cells ($2.8 \times 10^5 \pm 6.9 \times 10^4$ $CD8^+$ T cells as measured by FACS analysis) in the lung which was associated with a decrease in lung function (Figure 7A and B), and a >10% loss of body weight (data not shown). In contrast, CD4/CD8-depleted IRD

NIH-PA Author Manuscript

NIH-PA Author Manuscript

NIH-PA Author Manuscript

mice demonstrated less impairment of pulmonary function (Figure 7 A and B; $p<0.05$), and continued to gain body weight. Enhanced disease in the CD4-depleted IRD mand no body weight loss (data not shown). By week four post reconstitution, the CD4-depleted ice that retained $CD8^+$ T cell function was associated with obvious histological signs of inflammation and lung injury, which was quantified by a blinded pathologist (Figure 8A, B, and C), and increased pro-inflammatory cytokine production in the lung (Figure 9; $p<0.05$). These data demonstrated that in the absence of $CD4^+$ T cells, $CD8^+$ T cells caused significant inflammatory injury in this IRD model. However, the injurious response was delayed compared to the acute $CD4^+$ T cell-dependent injury, and importantly, $CD8^+$ T cell-mediated injury proceeded without the beneficial effect of organism clearance.

Discussion

PcP-related IRD is observed not only in non-HIV-infected patients who undergo immunosuppressive therapies followed by an immune-recovery phase, but also in HIV-infected patients following the initiation of HAART therapy and recovery of $CD4^+$ T cell function (34; 42). Using a murine model of IRD, the contribution of individual lymphocyte subsets was studied by selective depletion using specific monoclonal antibodies. Our results not only confirmed that $CD4^+$ T cells are critical for *P. carinii*-clearance (16; 30; 34; 39), but also demonstrated that they directly contribute to the severe lung injury associated with IRD. Furthermore our results show that $CD8^+$ T cells also play a dual role during PcP: an immune-modulatory role in the presence of $CD4^+$ T cells, and an inflammatory, non-protective role in the absence of $CD4^+$ T cells. Interestingly, the clinical reports of IRD have suggested that the PcP may be minimally symptomatic prior to immunorestitution, but following immunorestitution the degree of $CD4^+$ T cell recovery is directly related to the ultimate severity of IRD associated with PcP (42). Therefore, it is possible that dysregulation of the CD4-mediated anti-*P. carinii* immune response occurring following immune recovery leads to enhancement of immune-mediated lung injury, and the observed high rate of mortality. For example, it has been reported that CD4 function is restored more quickly than CD8 function following HAART treatment (11; 24). The lag in $CD8^+$ T cell recovery may result in less control over a pathological CD4 response associated with IRD, and cause a significant enhancement of lung injury, similar to what we have documented in CD8-depleted mice. Consistent with this hypothesis is a recent case-control study of newly diagnosed and anti-retroviral treated patients, demonstrating that patients who developed IRD had larger increases in percentage of $CD4^+$ T-cells as well as higher $CD4^+$ to $CD8^+$ T-cell ratios 12 weeks after initiation of therapy when compared to matched control patients who did not develop IRD after beginning HAART. (28) Given the potential severity of IRD in patients who present with PcP as their initial manifestation of AIDS, and our animal model data suggesting that a major contributor to IRD is the kinetics of return of $CD4^+$ and $CD8^+$ T-cells, we speculate that delaying institution of antiretroviral therapy for several weeks until the treatment of the PcP has been completed may reduce the incidence of PcP-associated IRD. A study which will test this hypothesis is underway through the National Institutes of Health AIDS Clinical Trials Group (ACTG protocol A5164).

Our experiments highlight the contribution of T lymphocytes to immune-mediated lung damage during PcP-related IRD. Consistent with previously published studies (16; 17; 30;

NIH-PA Author Manuscript

NIH-PA Author Manuscript

NIH-PA Author Manuscript

33; 39), our studies show that $CD4^+$ T cells are absolutely essential to clear the *P. carinii* infection. It is possible that features of CD4 function which are essential for *Pneumocystis carinii* clearance are also responsible for inflammatory lung injury. Alternatively, certain aspects of CD4 function may mediate clearance, while other aspects drive lung injury. In either case, further understanding of CD4 function and the mechanisms controlling the intensity and duration of their responses are needed.

Our murine IRD model has allowed us to study the effect $CD8^+$ T cells have on *P. carinii* clearance and pathophysiology in the presence or absence of $CD4^+$ T cells, something that has not been done before. Based on our prior work demonstrating that $CD8^+$ T cells mediate inflammation and injury in a CD4-depleted mouse model of PcP (39; 41), we hypothesized that IRD-related injury was the result of the combined CD4-and CD8-mediated injurious response, and that the depletion of $CD8^+$ T cells would alleviate some of this injury. However, depleting $CD8^+$ T cells appeared to enhance the CD4-mediated lung injury that is characteristic of IRD. $CD8^+$ T cell depleted mice had reduced lung function compared to non-depleted mice, and more often appeared moribund. Interestingly, the more severe IRD observed when $CD8^+$ T cells were depleted was associated with higher IFN-γ levels in the lungs at seven days post-reconstitution. Intracellular staining for IFN-γ revealed that depletion of $CD8^+$ T cells resulted in more $CD4^+$/IFN-γ^+ cells in the lungs, suggesting that $CD8^+$ T cells can modulate the $CD4^+$ T cell response during PcP-related IRD. Since IFN-γ is one of the hallmarks of T_H1-mediated immune responses (6; 27), $CD8^+$ T cells are likely regulating the intensity or polarity of the $CD4^+$ T cell response. The number of $CD4^+$/IFN-γ^+ T cells in the CD8-depleted group was greater at day 6 post-reconstitution (see Figure 6C), suggesting that differences in IFN-γ could be due to either differences in the level of IFN production by individual $CD4^+$ T cells, or differences in the number of IFN-γ producing $CD4^+$ T cells. $CD8^+$ T cells have been reported to act as negative regulators of inflammation in certain models of disease. For example, a regulatory role for $CD8^+$ T cells in controlling $CD4^+$ T cell mediated inflammatory response has been described in a mouse model of *Mycoplasma pulmonis* respiratory disease (19). It is apparent that a similar phenomenon is occurring in our studies that merits further study. One possible explanation for the observed regulatory effect of $CD8^+$ T cells is they might be somehow affecting $CD4^+$ helper T cell function. It is also possible that a specific subset of $CD8^+$ T cells regulates the immune response in an antigen specific manner. These possibilities are subjects of further study.

Our studies suggest an important role for IFN-γ in initiating and regulating inflammatory response to PcP in this mouse model. In the two groups that show severe $CD4^+$ T cell mediated inflammation and lung injury (non-depleted and $CD8^+$ T cell depleted IRD groups), elevated IFN-γ levels were detected at 9 DPR. The role of IFN-γ in regulating the immune response to *P. carinii* has been described before. It has been shown to play a role in TNF-α- and L-arginine mediated killing of *P. carinii* by rat alveolar macrophages (10). However, even though it collaborates with TNF-α in anti-*P. carinii* defenses, it is not absolutely necessary and sufficient for *P. carinii*-clearance (12). Kolls et al. have shown that expression of IFN-γ through an intracellular delivery system can prime $CD8^+$ T cells to protect CD4-depleted mice against subsequent challenge with *P. carinii* (20). In contrast, IFN-γ has also been shown to play a more regulatory role in controlling the inflammation

NIH-PA Author Manuscript

NIH-PA Author Manuscript

NIH-PA Author Manuscript

associated with *P. carinii* infection (12). In a bone marrow transplantation mouse model, treatment with anti-IFN-γ antibodies worsened *P. carinii*induced pneumonitis (13), and in a model of PcP-related IRD the lack of IFN appeared to delay the resolution of pulmonary inflammation (12). Our results suggest that IFN-γ may play a role in enhancing the CD4-mediated inflammatory response important for the generation of PcP-related IRD. Since both anti and pro-inflammatory roles for IFN-γ have been demonstrated, the timing and magnitude of the IFN-γ response may dictate the specific role it plays during PcP-related IRD. We are currently investigating this role further.

It must be noted that while the studies presented herein were designed to focus specifically on the role of T cell subsets during PcP-related IRD, other variables also affect the ultimate outcome of disease. For example, the intensity of the *P. carinii* infection at the time of immune reconstitution is critical. In some experiments we have performed, a higher *P. carinii* burden led to a very severe IRD in both CD8-depleted and non-depleted mice, resulting in an altered time frame of disease and/or lethal IRD, and obscuring the immunomodulatory effects of $CD8^+$ T cells. In other experiments, a very light *P. carinii* burden at the time of reconstitution has resulted in little lung injury in either group. Furthermore, we have noted an alteration in the time course of disease onset in some experiments, possibly also related to the *P. carinii* burden, or alternatively to the quality of the donor lymphocytes. Thus, we have found that the time course of PcP-related IRD is very dependent upon the intensity of infection, and the number and composition of the donor lymphocytes. Future experiments will need to examine a more detailed time course of disease progression.

Our studies also suggest that $CD8^+$ T cells contribute to a delayed injurious immune response in the absence of $CD4^+$ T cells. All the parameters of lung injury and inflammation are better in $CD8^+/CD4^+$ T cell double depleted mice as compared to mice depleted of only $CD4^+$ T cells, suggesting an inflammatory role for the $CD8^+$ T cells. It will be interesting to study whether $CD8^+$ T cell mediated inflammation observed in PcP lungs is MHC class I restricted, which antigen of *P. carinii* is recognized by $CD8^+$ T cells, and how *P. carinii* antigens are presented to the $CD8^+$ T cells since *P. carinii* is not an intracellular pathogen.

We have demonstrated dual roles for both $CD4^+$ and $CD8^+$ T cells during PcP-related IRD. $CD4^+$ T cells were required for *P. carinii* clearance, but also induced the severe pulmonary inflammatory syndrome associated with IRD. In the absence of $CD4^+$ T cells, $CD8^+$ T cells were responsible for a delayed inflammatory response that was not capable of clearing the *P. carinii* infection, but did cause significant lung injury. However, when $CD4^+$ T cells were present, $CD8^+$ T cells played an immunomodulatory function by limiting the intensity and/or altering the polarity of the injurious CD4 response.

Based on this study and our previously published experiments (2; 14; 39; 40) we propose the following conceptual framework to think about how T-cells affect the outcome of PcP. We suggest that the overall inflammatory response and outcome of infection with *P. carinii* is dependent on the balance between $CD4^+$ and $CD8^+$ T- cells. With a balanced or physiologic response, as would be seen in the normal host, infection is easily cleared with minimal inflammation and little apparent “disease” (2; 14). With a $CD4^+$ T-cell dominant response in

NIH-PA Author Manuscript

NIH-PA Author Manuscript

NIH-PA Author Manuscript

the absence of adequate $CD8^+$ T-cell suppression, e.g. as might be seen in IRD, infection is rapidly cleared but at the expense of excessive inflammation and bystander injury to the lung (as shown in this study). Finally, with a $CD8^+$ T-cell dominant response in the absence of adequate $CD4^+$ T-cell help (39; 40), e.g. as might be seen in patients receiving chemotherapy or in AIDS patients with high $CD8^+$ to $CD4^+$ T-cell ratios, there is futile inflammation with bystander injury to the lung and failure to clear infection. A better understanding of these T-cell effects should allow for improved therapy of PcP.

Acknowledgments

We wish to thank Stephanie Campbell, Margaret Chovaniec and Greg Roat for technical assistance. This work was supported by Public Health Service grants HL-64559 and PO1 HL71659-01 from the National Heart, Lung, and Blood Institute.

References

1. Amdur MO, Mead J. Mechanics of respiration in unanesthetized guinea pigs. Am J Physiol. 1958; 192:364–368. [PubMed: 13508884]
2. An CL, Gigliotti F, Harmsen AG. Exposure of immunocompetent adult mice to *Pneumocystis carinii* f. sp. muris by cohousing: growth of P. *carinii* f. sp. muris and host immune response. Infect Immun. 2003; 71:2065–2070. [PubMed: 12654827]
3. Beck JM, Newbury RL, Palmer BE, Warnock ML, Byrd PK, Kaltreider HB. Role of $CD8^+$ lymphocytes in host defense against *Pneumocystis carinii* in mice. J Lab Clin Med. 1996; 128:477–487. [PubMed: 8900290]
4. Benfield TL, Helweg-Larsen J, Bang D, Junge J, Lundgren JD. Prognostic Markers of Short-term Mortality in AIDS-Associated *Pneumocystis carinii* Pneumonia. Chest. 2001; 119:844–851. [PubMed: 11243967]
5. Bergmann KC, Lachmann B, Noack K. Lung mechanics in orally immunized mice after aerolized exposure to influenza virus. Respiration. 1984; 46:218–221. [PubMed: 6494618]
6. Billiau A. Interferon-gamma: biology and role in pathogenesis. Adv Immunol. 1996; 62:61–130. [PubMed: 8781267]
7. Chen W, Havell EA, Harmsen AG. Importance of endogenous tumor necrosis factor alpha and gamma interferon in host resistance against *Pneumocystis carinii* infection. Infect Immun. 1992; 60:1279–1284. [PubMed: 1548057]
8. Chen W, Havell EA, Moldawer LL, McIntyre KW, Chizzonite RA, Harmsen AG. Interleukin 1: an important mediator of host resistance against *Pneumocystis carinii*. J Exp Med. 1992; 176:713–718. [PubMed: 1387414]
9. Cheng VC, Yuen KY, Chan WM, Wong SS, Ma ES, Chan RM. Immunorestitution disease involving the innate and adaptive response. Clin Infect Dis. 2000; 30:882–892. [PubMed: 10880300]
10. Downing JF, Kachel DL, Pasula R, Martin WJ. Gamma interferon stimulates rat alveolar macrophages to kill *Pneumocystis carinii* by L-arginine- and tumor necrosis factor-dependent mechanisms. Infect Immun. 1999; 67:1347–1352. [PubMed: 10024581]
11. Evans TG, Bonnez W, Soucier HR, Fitzgerald T, Gibbons DC, Reichman RC. Highly active antiretroviral therapy results in a decrease in $CD8^+$ T cell activation and preferential reconstitution of the peripheral $CD4^+$ T cell population with memory rather than naive cells. Antiviral Res. 1998; 39:163–173. [PubMed: 9833957]
12. Garvy BA, Ezekowitz RA, Harmsen AG. Role of gamma interferon in the host immune and inflammatory responses to *Pneumocystis carinii* infection. Infect Immun. 1997; 65:373–379. [PubMed: 9009285]
13. Garvy BA, Gigliotti F, Harmsen AG. Neutralization of interferon-gamma exacerbates *Pneumocystis*-driven interstitial pneumonitis after bone marrow transplantation in mice. J Clin Invest. 1997; 99:1637–1644. [PubMed: 9120007]

NIH-PA Author Manuscript

NIH-PA Author Manuscript

NIH-PA Author Manuscript

14. Gigliotti F, Harmsen AG, Wright TW. Characterization of transmission of *Pneumocystis carinii* f. sp. muris through immunocompetent BALB/c mice. Infect Immun. 2003; 71:3852–3856. [PubMed: 12819069]
15. Hanano R, Kaufmann SH. *Pneumocystis carinii* and the immune response in disease. Trends Microbiol. 1998; 6:71–75. [PubMed: 9507642]
16. Hanano R, Reifenberg K, Kaufmann SH. Naturally acquired *Pneumocystis carinii* pneumonia in gene disruption mutant mice: roles of distinct T-cell populations in infection. Infect Immun. 1996; 64:3201–3209. [PubMed: 8757854]
17. Harmsen AG, Stankiewicz M. Requirement for $CD4^+$ cells in resistance to *Pneumocystis carinii* pneumonia in mice. J Exp Med. 1990; 172:937–945. [PubMed: 2117637]
18. Hori S, Carvalho TL, Demengeot J. CD25+$CD4^+$ regulatory T cells suppress $CD4^+$ T cell-mediated pulmonary hyperinflammation driven by *Pneumocystis carinii* in immunodeficient mice. Eur J Immunol. 2002; 32:1282–1291. [PubMed: 11981815]
19. Jones HP, Tabor L, Sun X, Woolard MD, Simecka JW. Depletion of $CD8^+$ T cells exacerbates $CD4^+$ Th cell-associated inflammatory lesions during murine mycoplasma respiratory disease. J Immunol. 2002; 168:3493–3501. [PubMed: 11907110]
20. Kolls JK, Habetz S, Shean MK, Vazquez C, Brown JA, Lei D, Schwarzenberger P, Ye P, Nelson S, Summer WR, Shellito JE. IFN-gamma and $CD8^+$ T cells restore host defenses against *Pneumocystis carinii* in mice depleted of $CD4^+$ T cells. J Immunol. 1999; 162:2890–2894. [PubMed: 10072538]
21. Koval CE, Gigliotti F, Nevins D, Demeter LM. Immune reconstitution syndrome after successful treatment of *Pneumocystis carinii* pneumonia in a man with human immunodeficiency virus type 1 infection. Clin Infect Dis. 2002; 35:491–493. [PubMed: 12145736]
22. Lee LH, Gigliotti F, Wright TW, Simpson-Haidaris PJ, Weinberg GA, Haidaris CG. Molecular characterization of KEX1, a kexin-like protease in mouse *Pneumocystis carinii*. Gene. 2000; 242:141–150. [PubMed: 10721706]
23. Limper AH, Offord KP, Smith TF, Martin WJ. *Pneumocystis carinii* pneumonia. Differences in lung parasite number and inflammation in patients with and without AIDS. Am Rev Respir Dis. 1989; 140:1204–1209. [PubMed: 2817582]
24. Marchetti G, Meroni L, Molteni C, Bandera A, Franzetti F, Galli M, Moroni M, Clerici M, Gori A. Interleukin-2 immunotherapy exerts a differential effect on CD4 and CD8 T cell dynamics. AIDS. 2004; 18:211–216. [PubMed: 15075538]
25. McAllister F, Steele C, Zheng M, Young E, Shellito JE, Marrero L, Kolls JK. T cytotoxic-1 $CD8^+$ T cells are effector cells against *Pneumocystis* in mice. J Immunol. 2004; 172:1132–1138. [PubMed: 14707088]
26. Mussini C, Pinti M, Borghi V, Nasi M, Amorico G, Monterastelli E, Moretti L, Troiano L, Esposito R, Cossarizza A. Features of 'CD4-exploders', HIVpositive patients with an optimal immune reconstitution after potent antiretroviral therapy. AIDS. 2002; 16:1609–1616. [PubMed: 12172082]
27. Paludan SR. Synergistic action of pro-inflammatory agents: cellular and molecular aspects. J Leukoc Biol. 2000; 67:18–25. [PubMed: 10647993]
28. Robertson J, Meier M, Wall J, Ying J, Fichtenbaum CJ. Immune reconstitution syndrome in HIV: validating a case definition and identifying clinical predictors in persons initiating antiretroviral therapy. Clin Infect Dis. 2006; 42:1639–1646. [PubMed: 16652323]
29. Rosen MJ. Pulmonary complications of HIV infection. Mt Sinai J Med. 1992; 59:263–270. [PubMed: 1603116]
30. Roths JB, Sidman CL. Both immunity and hyperresponsiveness to *Pneumocystis carinii* result from transfer of $CD4^+$ but not $CD8^+$ T cells into severe combined immunodeficiency mice. J Clin Invest. 1992; 90:673–678. [PubMed: 1353767]
31. Roths JB, Sidman CL. Single and combined humoral and cell-mediated immunotherapy of *Pneumocystis carinii* pneumonia in immunodeficient scid mice. Infect Immun. 1993; 61:1641–1649. [PubMed: 8478052]

NIH-PA Author Manuscript

NIH-PA Author Manuscript

NIH-PA Author Manuscript

32. Ruan S, Tate C, Lee JJ, Ritter T, Kolls JK, Shellito JE. Local delivery of the viral interleukin-10 gene suppresses tissue inflammation in murine *Pneumocystis carinii* infection. Infect Immun. 2002; 70:6107–6113. [PubMed: 12379687]
33. Shellito J, Suzara VV, Blumenfeld W, Beck JM, Steger HJ, Ermak TH. A new model of *Pneumocystis carinii* infection in mice selectively depleted of helper T lymphocytes. J Clin Invest. 1990; 85:1686–1693. [PubMed: 2139668]
34. Thomas CF Jr, Limper AH. *Pneumocystis* pneumonia. N Engl J Med. 2004; 350:2487–2498. [PubMed: 15190141]
35. Vargas SL, Hughes WT, Santolaya ME, Ulloa AV, Ponce CA, Cabrera CE, Cumsille F, Gigliotti F. Search for primary infection by *Pneumocystis carinii* in a cohort of normal, healthy infants. Clin Infect Dis. 2001; 32:855–861. [PubMed: 11247708]
36. Vestbo J, Nielsen TL, Junge J, Lundgren JD. Amount of *Pneumocystis carinii* and degree of acute lung inflammation in HIV-associated P *carinii* pneumonia. Chest. 1993; 104:109–113. [PubMed: 8100757]
37. Walzer PD, Perl DP, Krogstad DJ, Rawson PG, Schultz MG. *Pneumocystis carinii* penumonia in the United States. Epidemiologic, diagnostic, and clinical features. Ann Intern Med. 1974; 80:83–93. [PubMed: 4589515]
38. Wang J, Gigliotti F, Maggirwar S, Johnston C, Finkelstein JN, Wright TW. *Pneumocystis* Activates the NF-κB Signaling Pathway in Alveolar Epithelial Cells. Infect Immun. 2005; 73:2766–2777. [PubMed: 15845480]
39. Wright TW, Gigliotti F, Finkelstein JN, McBride JT, An CL, Harmsen AG. Immune-mediated inflammation directly impairs pulmonary function, contributing to the pathogenesis of *Pneumocystis carinii* pneumonia. J Clin Invest. 1999; 104:1307–1317. [PubMed: 10545529]
40. Wright TW, Notter RH, Wang Z, Harmsen AG, Gigliotti F. Pulmonary inflammation disrupts surfactant function during *Pneumocystis carinii* pneumonia. Infect Immun. 2001; 69:758–764. [PubMed: 11159965]
41. Wright TW, Pryhuber GS, Chess PR, Wang Z, Notter RH, Gigliotti F. TNF receptor signaling contributes to chemokine secretion, inflammation, and respiratory deficits during *Pneumocystis* pneumonia. J Immunol. 2004; 172:2511–2521. [PubMed: 14764724]
42. Wu AK, Cheng VC, Tang BS, Hung IF, Lee RA, Hui DS, Yuen KY. The unmasking of *Pneumocystis* jiroveci pneumonia during reversal of immunosuppression: case reports and literature review. BMC Infect Dis. 2004; 4:57. [PubMed: 15588295]

NIH-PA Author Manuscript

NIH-PA Author Manuscript

NIH-PA Author Manuscript

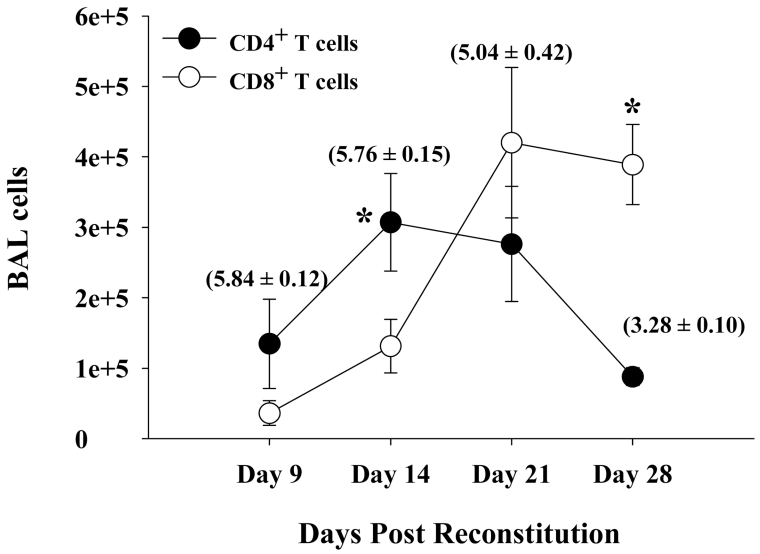

Figure 1. Number of CD4$^+$ and CD8$^+$ T cells in the BAL of IRD mice

Cells were recovered from the lungs of *Pneumocystis carinii* infected SCID mice by BAL at various times following immune reconstitution. The percentage of CD4$^+$ and CD8$^+$ T cells present in the BAL was then determined by FACS analysis, and were used to calculate numbers of CD4$^+$ or CD8$^+$ T cells from total cell counts. Closed circles represent CD4$^+$ T cells and open circles represent CD8$^+$ T cells. Values in bracket above each CD4$^+$ time point shows *Pneumocystis carinii* burden expressed as Log10(kexin DNA copies) at that particular data point as assessed by quantitative real-time PCR and was measured as described in Materials and Methods. Each data point is expressed as the arithmetic mean ± 1 SEM (n= 4-7 mice at each time point; * denotes p≤0.05).

NIH-PA Author Manuscript
NIH-PA Author Manuscript
NIH-PA Author Manuscript

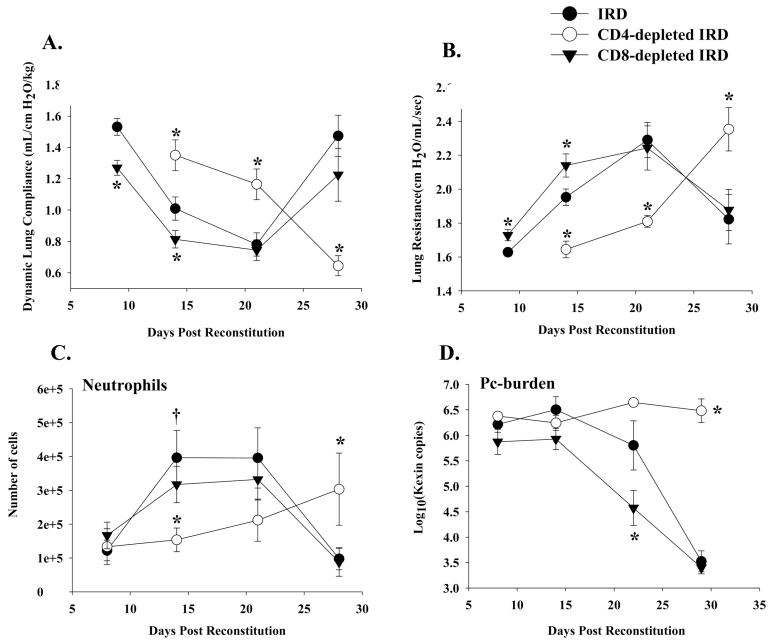

Figure 2. Effect of lymphocyte subsets on lung function during PcP in IRD mice

Pulmonary function testing was carried out on Pc-infected IRD mice at 9, 14, 21 and 28 days post-immune reconstitution. Lung compliance (Panel A), and resistance (Panel B) measurements were taken on non-depleted (closed circles), CD4-depleted (open circles) and CD8-depleted (closed triangles) IRD mice. Panel C shows PMN numbers in the BAL fluid of experimental mice, and Panel D shows *Pneumocystis carinii*-burden expressed as Log_{10}(kexin DNA copies) as measured by quantitative real time PCR. The results were pooled data from three independent experiments, and each data point is the arithmetic mean ± 1 SEM (n= 8-16 mice for all groups at all time points except CD4-depleted mice at day 21 (n= 3). *P<0.05 as compared to non-depleted IRD mice.

NIH-PA Author Manuscript

NIH-PA Author Manuscript

NIH-PA Author Manuscript

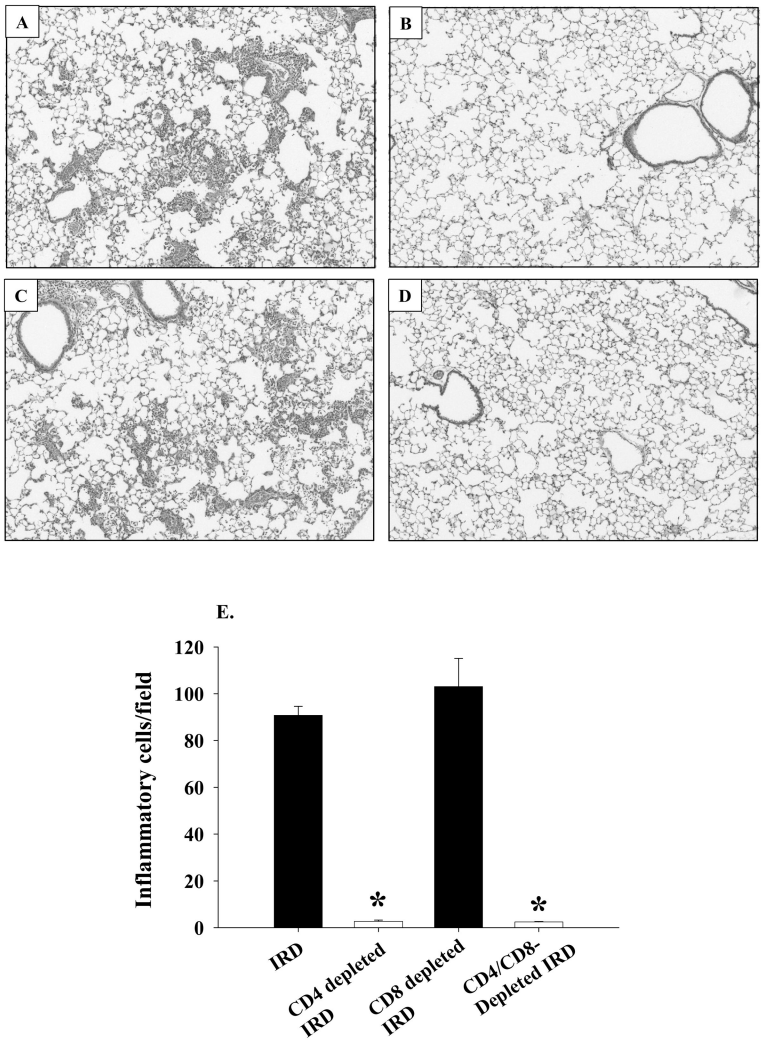

Figure 3. Histopathology of PcP in IRD mice

At 14 days post-reconstitution lungs from non-depleted (Panel A), CD4-depleted (Panel B), CD8-depleted (Panel C), or CD4 and CD8-depleted (Panel D) IRD mice were inflation fixed with 10% buffered formalin. Four-micron sections were stained with hematoxylin and eosin and photographed at X100 magnification. The number of inflammatory cells per field were determined as described in the Materials and Methods section, and are represented as a bar graph in Panel E. Bars represent arithmetic mean ± 1 SEM (*$P < 0.05$ as compared to non-depleted group).

NIH-PA Author Manuscript

NIH-PA Author Manuscript

NIH-PA Author Manuscript

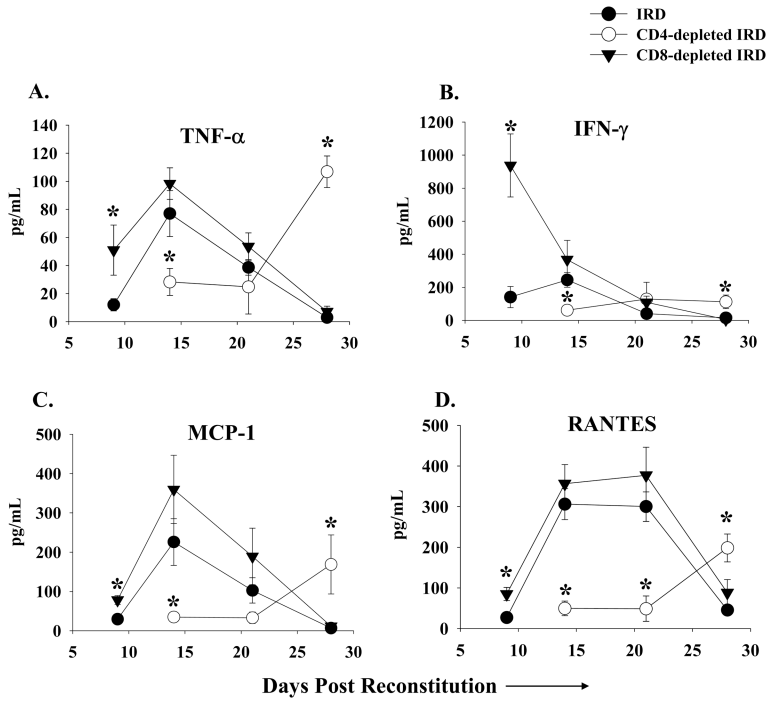

Figure 4. Cytokine/chemokine levels in the BAL of *Pneumocystis carinii* infected IRD mice

TNF-α, INF-γ, MCP-1, and RANTES protein levels were measured in the BAL of non-depleted (closed circles), CD4-depleted (open circles), and CD8-depleted (closed triangles) IRD mice. Each data point represents the arithmetic mean of the combined data of three independent experiments ± 1 SEM. (n> 7 mice for each data point except CD4-depleted mice at day 21 (n= 3)). *P<0.05 as compared to non-depleted IRD mice.

NIH-PA Author Manuscript

NIH-PA Author Manuscript

NIH-PA Author Manuscript

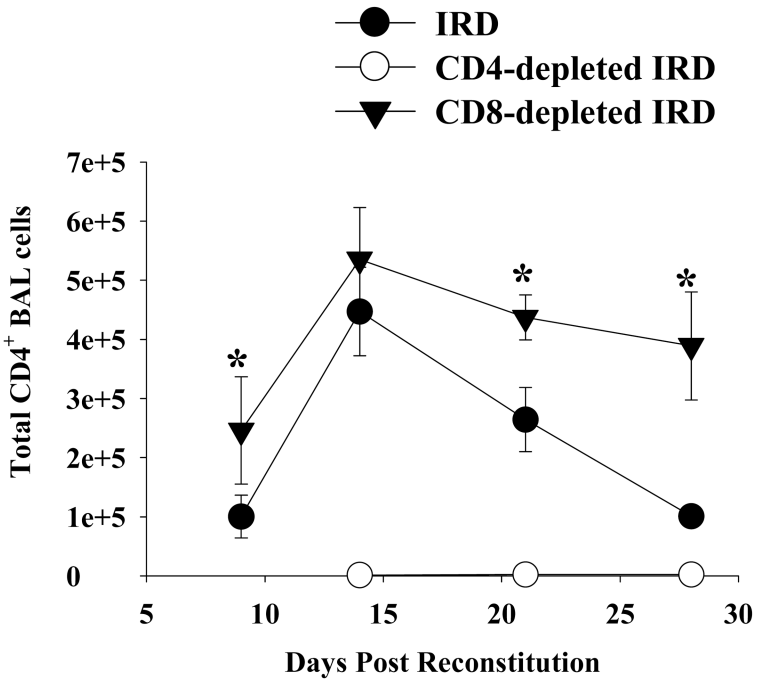

Figure 5. CD4$^+$ T cells in the BAL of IRD mice

Cells were recovered from non-depleted (closed circles), CD4-depleted (open circles), and CD8-depleted (closed triangles) IRD mice by BAL, and then stained with fluorescent conjugated anti-CD4 antibodies. FACS analysis was used to determine total number of CD4$^+$ T cells. The data represents the arithmetic mean of samples pooled from three independent experiments ± 1 SEM. (n= 5-14 mice for all groups at all time points, except for CD4-depleted mice at day 21 (n=3)). *P<0.05 as compared to non-depleted IRD mice.

NIH-PA Author Manuscript

NIH-PA Author Manuscript

NIH-PA Author Manuscript

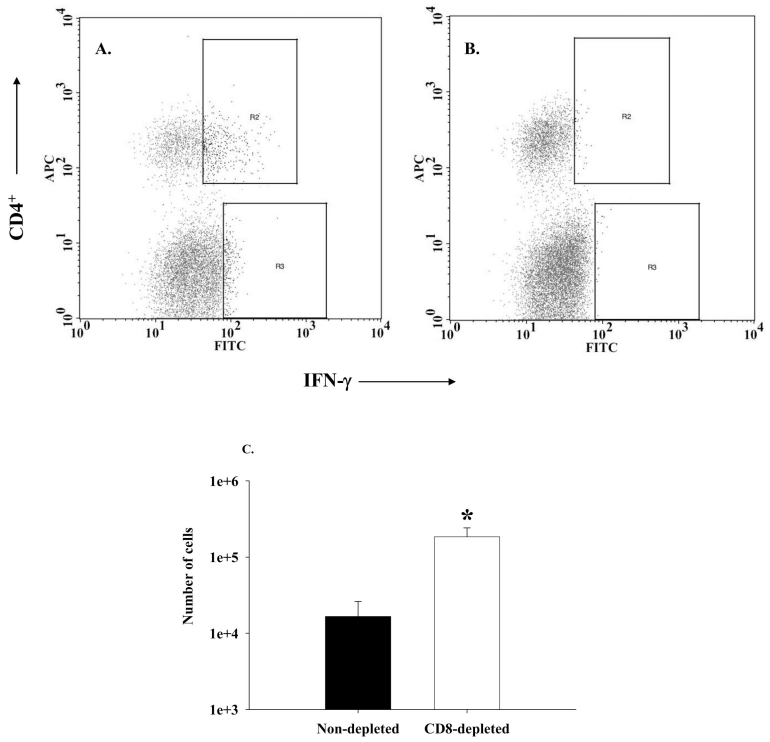

Figure 6. CD4$^+$ IFN-γ$^+$ T cells are readily detected in the lung tissue of experimental mice

Lung cells were isolated from experimental mice sacrificed on the seventh day after immune reconstitution, stimulated with PMA and ionomycin, and stained with fluorescent MAbs against the following surface markers: CD4 (APC) and CD8 (PerCP) as well as intracellular IFN-γ (FITC). Results of pooled cells from CD8-depleted IRD mice are shown in Panel A. The same cells pre-treated with 10 μg of unlabeled anti-IFN-γ shows nearly complete blocking of IFN staining. The percentage of CD4$^+$ IFN-γ$^+$ cells [cells in the gate R2] from a similar plot for each sample were used to calculate total number of IFN-γ -producing CD4$^+$ T cells in that sample, and the results are shown in Panel C. Bars represent arithmetic means of three samples and error bars represent 1 SEM *$p<0.05$..

NIH-PA Author Manuscript
NIH-PA Author Manuscript
NIH-PA Author Manuscript

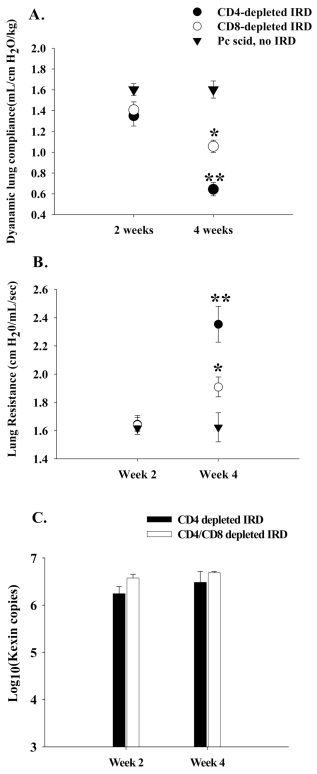

Figure 7. Effect of CD8$^+$ T cells on lung function during PcP in CD4-depleted IRD mice

Pulmonary function testing was performed on *Pneumocystis carinii*-infected IRD mice in the absence of CD4$^+$ T cells. During weeks 2 and 4 post-immune reconstitution, lung compliance (Panel A), and resistance (Panel B) measurements were taken on CD4-depleted (closed circles) and CD4/CD8-depleted (open circles) IRD mice. *Pneumocystis carinii*-infected mice that were not immune reconstituted served as controls (closed triangles).. *P. carinii* burden for the CD4-depleted mice are shown in Panel C. The results were pooled data from three independent experiments, and each data point is the arithmetic mean ± 1 SEM (n= 8-11 mice for each IRD group at each time point; n= 3 mice at each time point for non-reconstituted mice). *p<0.05 as compared to non-reconstituted, infected mice. **p<0.05 as compared to both non-reconstituted and CD4/CD8-depleted IRD mice.

NIH-PA Author Manuscript

NIH-PA Author Manuscript

NIH-PA Author Manuscript

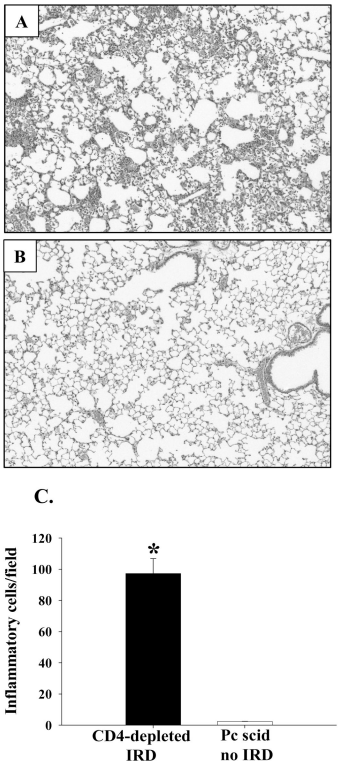

Figure 8. Histopathology of PcP in CD4-depleted IRD mice

At 4 weeks post-reconstitution, lungs from CD4-depleted IRD mice (Panel A), and non-reconstituted *Pneumocystis carinii*-infected mice (Panel B) were inflation fixed. Four-micron sections were then stained with hematoxylin and eosin and photographed at X100 magnification. The number of inflammatory cells per field were determined as described in the Materials and Methods section, and are represented as a bar graph in Panel C. Bars represent arithmetic mean ± 1 SEM (*$P < 0.05$ as compared to infected but not-reconstituted group).

NIH-PA Author Manuscript

NIH-PA Author Manuscript

NIH-PA Author Manuscript

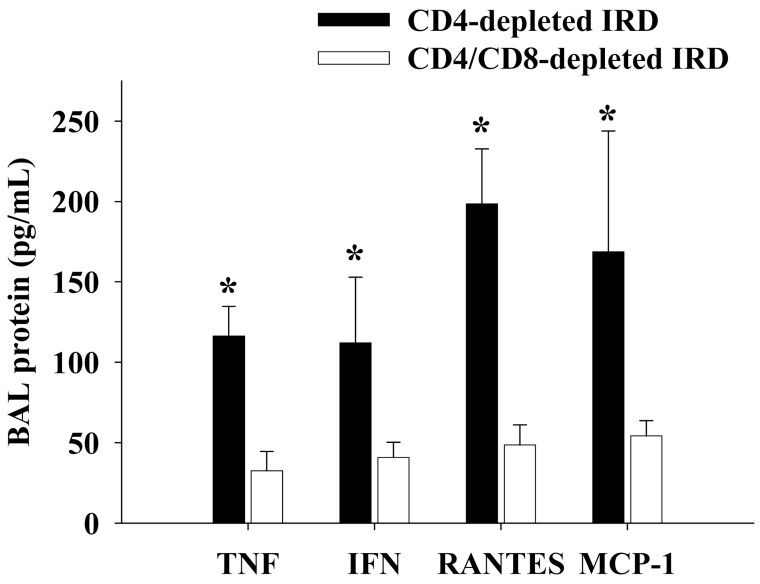

Figure 9. Effect of CD8$^+$ T cells on cytokine/chemokine levels in the BAL during PcP in CD4-depleted IRD mice

TNF-α, INF-γ, MCP-1, and RANTES protein levels were measured in the BAL of CD4-depleted (black bars), and CD4/CD8-depleted (white bars) IRD mice during week 4 post-reconstitution. Each data point represents the arithmetic mean of the combined data of three independent experiments ± 1 SEM. (n= 6-10 mice for each data point). *P<0.05 as compared to CD4/CD8-depleted IRD mice.